

Behavior of earth dam during reservoir filling and earthquake action, dam in Slovenia

Ljupcho Petkovski, Stevcho Mitovski, Frosina Panovska

Faculty of Civil Engineering, Ss. Cyril and Methodius University in Skopje, North Macedonia

ABSTRACT: In the static analysis of the earth zoned dam in Slovenia, for the state of rapid filling of the reservoir and lowering of the level for remediation of the dam, up to the state of long-term maintenance at normal level, which is a pre-earthquake state, an elastoplastic model with variable modulus of elasticity was used, for the local materials in the dam body. The analysis was performed in drained conditions with effective stresses, using combined mechanical and seepage analysis in the time domain. Criterion for calibration of nonlinear elastic material parameters is the condition that the horizontal displacements in the dam crest, for the condition of the first filling of the reservoir, are approximately the same with the measured values, i.e. about -120 mm in the downstream direction. The key conclusion from the static analysis is that the embankment dam, with the adopted geometry and composition of materials, possesses satisfactory static stability. In the analysis of the dynamic response of the dam, a nonlinear model is applied (equivalent linear analysis with inelastic material parameters), where the local materials are approximated with a variable maximum shear modulus. Permanent displacements during seismic excitation are determined by dynamic deformation analysis, where from the difference of the effective stresses in two successive time steps, incremental forces are determined, which result in corresponding deformations. The dynamic analysis confirms the seismic resistance of the embankment dam in the action of a design earthquake with PGA of 0.30 g, i.e. there is no danger of rapid and uncontrolled reservoir emptying, because the crest settlements from dynamic inertial forces for the duration of the earthquake are 1.1 m, apropos are much lower than the height above the normal level in the reservoir till dam crest, which is 3.2 m.

1 MODEL OF THE DAM AND MATERIAL PARAMETERS FOR STRUCTURAL ANALYSIS

1.1 Basic characteristics of the analyzed dam

The representative cross-section, the parameters of the local materials for the embankment dam in Slovenia and the measured values from the dam monitoring are taken from the available data base [1]. The earth zoned dam with a clay core was built in 1985. It is founded on a rock foundation of Eocene flysch, which is practically waterproof and with high stiffness. The basic geometric characteristics of the dam and reservoir, Figure 1, are the following: crest elevation at 102.0 m.a.s.l., elevation of rock foundation 67.4 m.a.s.l., structural height 34.6 m, crest width 5.0 m, elevation at normal level 98.8 m.a.s.l. and elevation at minimum level 80.0 m.a.s.l.

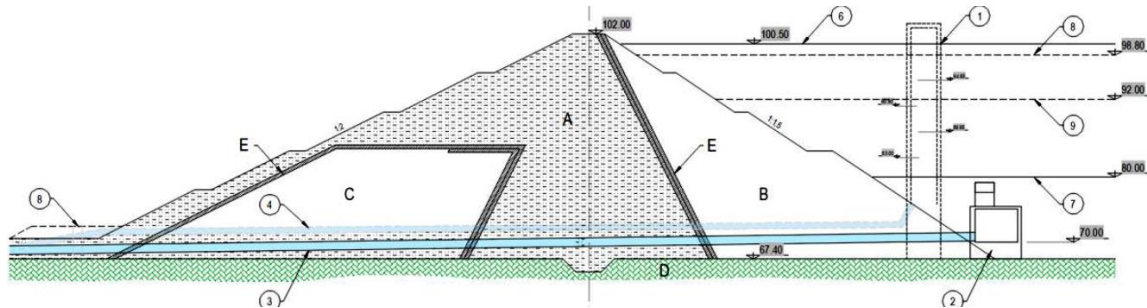


Figure 1. Representative cross-section of the earth dam.

1.2 Basic geomechanical parameters of the materials

The basic geomechanical parameters of the local materials are systematized in Table 1. The values from the available database are with a yellow background, and the other values are determined or assumed, according to the description of the materials.

Table 1. Material parameters.

Zone		A1	A2	B	C	D	Comment
dam structure		top of dam	core	up-stream part	down-stream part	bedrock	
material		gravel, silt	clayey silt	rockfill	rockfill and sand	Flysch	
γ_{spec}	kN/m ³	21.0	19.5	24.0	24.0	25.0	specific unit weight
γ_{dry}	kN/m ³	16.4	12.8	21.0	20.0	24.0	dry unit weight
n		0.219	0.344	0.125	0.167	0.040	void
e		0.280	0.523	0.143	0.200	0.042	void ratio
ω_{sat}	%	13.1	26.3	5.8	8.2	1.6	saturated wetness
$\omega < \omega_{sat}$	%	13.0	26.0	3.0	7.0	1.5	natural wetness
γ_{sat}	kN/m ³	18.5	16.2	22.2	21.6	24.4	saturated unit weight
γ	kN/m ³	18.5	16.1	21.6	21.4	24.4	natural unit weight
φ	o	36.0	0.0	38.0	38.0	39.0	angle if internal friction
c or cu	kN/m ²	36.0	75.0	0.0	0.0	32.0	cohesion
k_s	m/s	1.0E-06	1.00E-09	1.0E-03	1.0E-04	1.0E-09	coefficient of permeability - secondly
k_d	m/d	8.6E-02	8.6E-05	8.6E+01	8.6E+00	8.6E-05	coefficient of permeability - daily

$K_0(\varphi)$		0.41	1.00	0.38	0.38	0.37	at-rest earth pressure coefficient
$\nu(K_0)$		0.29	0.50	0.28	0.28	0.27	Poisson coefficient
ν		0.35	0.45	0.30	0.30	0.25	Poisson coefficient
M_v	kN/m ²	15,000	5,000	50,000	50,000		modulus of compressibility
m_v		6.67E-05	2.00E-04	2.00E-05	2.00E-05		coefficient of compressibility
E	kN/m ²	9,346	1,318	37,143	37,143	620,000	Young's modulus of elasticity

1.3 Mathematical model of the dam

In the mathematical model for simulating the behavior of the earth dam during the filling of the reservoir and the earthquake action, Figure 2, four different local materials are provided in the body of the dam, while the rock foundation at the base below the dam is adopted as non-deformable zone (due to the large difference in the stiffness properties) and also waterproof (due to the low coefficient of permeability). The justification for such approximation is confirmed by comparing models with and without rock foundation, for the state of reservoir filling, whereby a negligible difference in the state of stresses and deformations in the dam body is ascertained. Therefore, in order to avoid the bulkiness of the numerical model and the possible negative impact in the numerical experiments, all further analyzes are conveyed with a mathematical model where the rock foundation is not included.

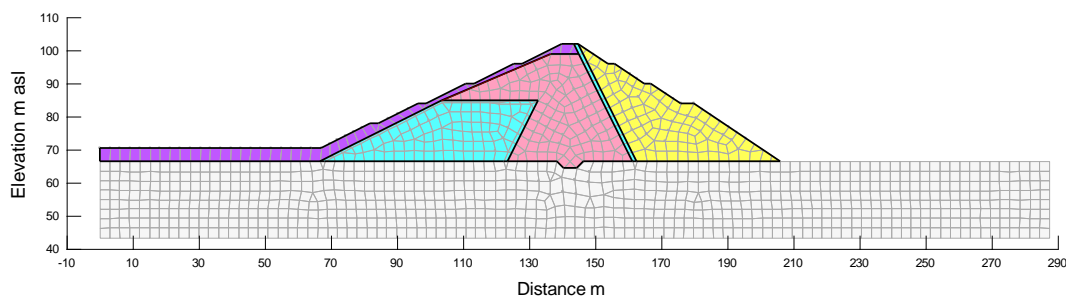


Figure 2. Mathematical model of the dam, discretized with 1,229 nodes и 1,147 elements.

2 SIMULATION OF DAM BEHAVIOR IN EXPLOITATION PERIOD

2.1 Stages of earth dam loading

The behavior of the dam in the service period is simulated with a mathematical model in real time domain, appropriate to the measured values from the technical monitoring. This ensures that the initial load state in the current load state is taken over from the previous stress state. The analyzes were performed using the effective stresses, apropos by tracking the increase and dissipation of the pore pressure with a coupled mechanical and hydraulic response with non-steady seepage in drained conditions.

The loading stages of the earth dam are systematized in Table 2. The monitoring of the dam behavior is simulated in a period of 33.54 years, from the beginning of the first filling of the reservoir, until the state of long-term maintenance at a normal level.

Table 2. Stages of loading of the earth dam.

Stage No.	description	from		to		dZ	Dt	dZ/Dt	Dt
		m asl	yyyy-mm-dd	masl	yyyy-mm-dd	m	days	m/d	years
1	first filling	81.84	1988-04-25	98.34	1990-04-17	16.50	722	0.023	1.977

2	to normal level	98.34	1990-04-17	98.80	1990-04-27	0.46	10	0.046	0.027
3	normal level	98.80	1990-04-27	98.80	2008-01-01	0.00	6,458	0.000	17.681
4	to emergency level	98.80	2008-01-01	92.00	2008-05-17	-6.80	137	-0.050	0.375
5	emergency level	92.00	2008-05-17	92.00	2018-05-17	0.00	3,652	0.000	9.999
6	to remediation level	92.00	2018-05-17	82.00	2018-12-06	-10.00	203	-0.049	0.556
7	remediation level	82.00	2018-12-06	82.00	2019-12-06	0.00	365	0.000	0.999
8	to normal level	82.00	2018-12-06	98.80	2019-11-08	16.80	337	0.050	0.923
9	normal level	98.80	2019-11-08	98.80	2020-11-07	0.00	365	0.000	0.999
10	earthquake	98.80	2020-11-07	98.80			12,249		33.54

2.2 Initial stress state prior to the first filling

The data from the monitoring of the dam are given for the first filling of the reservoir from elevation 81.84 m. Therefore, the initial stress state is determined for steady seepage through the dam for water level elevation dam at 81.84 m.a.s.l., Figure 3, by application of Seep/W program [2]. For this state of seepage pore pressure, the distribution of effective stresses in the dam body is determined, Figure 4, by application of Sigma/W program [3]. The coefficient of slope stability of the upstream slope is calculated with the realized stresses by application of program Slope/W [4] and is $F = 1.33$, apropos it is greater than the required 1.3, for temporary load.

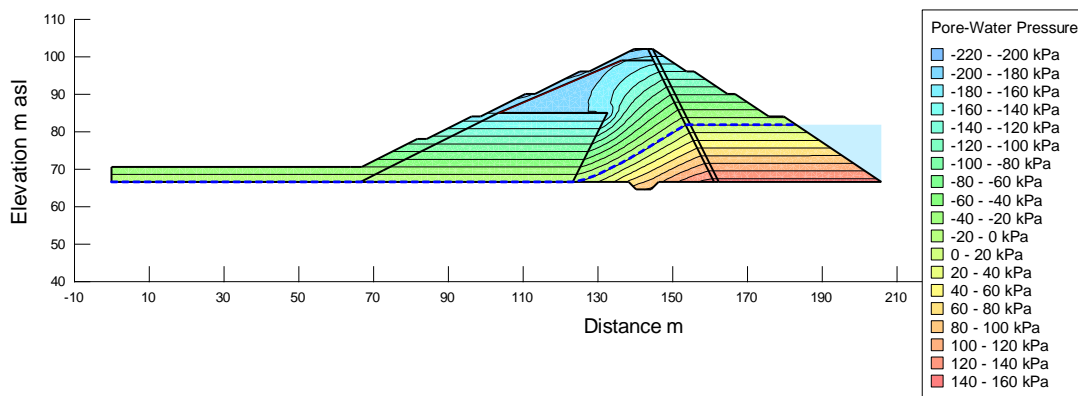


Figure 3. Initial state prior to the filling of the reservoir, distribution of pore pressure for steady seepage.

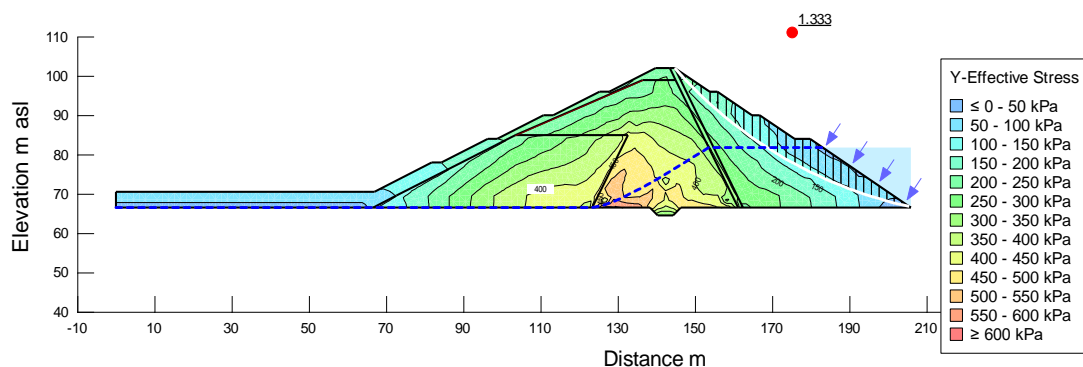


Figure 4. Initial state prior to the filling of the reservoir, distribution of vertical effective stress with coefficient of slope stability on the upstream slope $F=1.33$.

2.3 First filling of the reservoir and calibration of nonlinear material parameters

The first filling (or Stage 1) is simulated in 722 linear increments over a period of 722 days, according to the dynamics of the registered values from the technical monitoring, Figure 5.

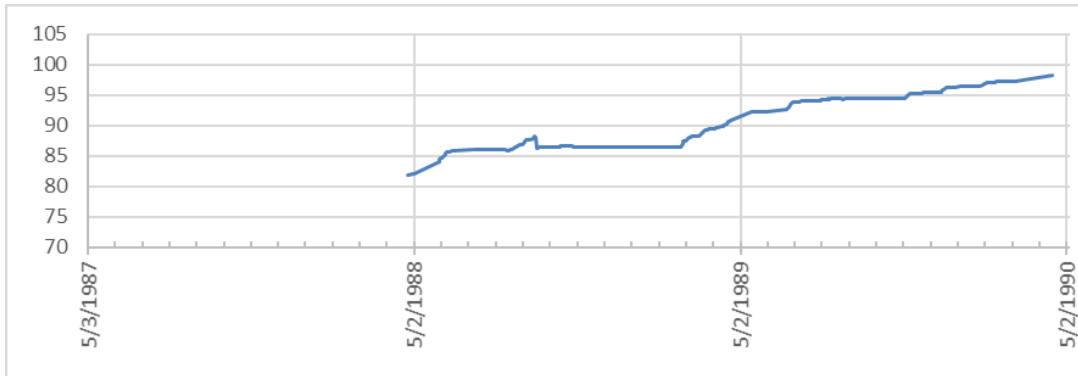


Figure 5. Dynamics of first filling of the reservoir, in m asl.

In the static analysis, for the local materials in the dam body, an elastoplastic model with variable modulus of elasticity $E = E(\sigma_y')$, Figure 6, with calibrated elastic parameters, is applied. Criterion for calibration is the condition that the horizontal displacements in the dam crest, for the state of the first filling of the reservoir, to be approximately same with the measured values, figure 7, i.e. about -120 mm in the downstream direction.

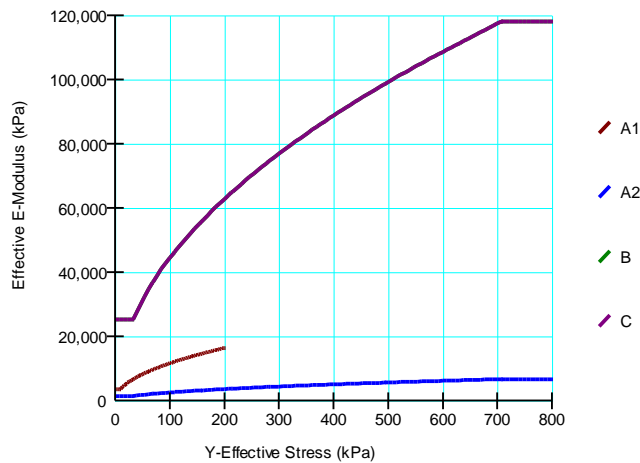


Figure 6. Calibrated values for variable elasticity modulus $E=E(\sigma_y')$ for the local materials in the dam body.

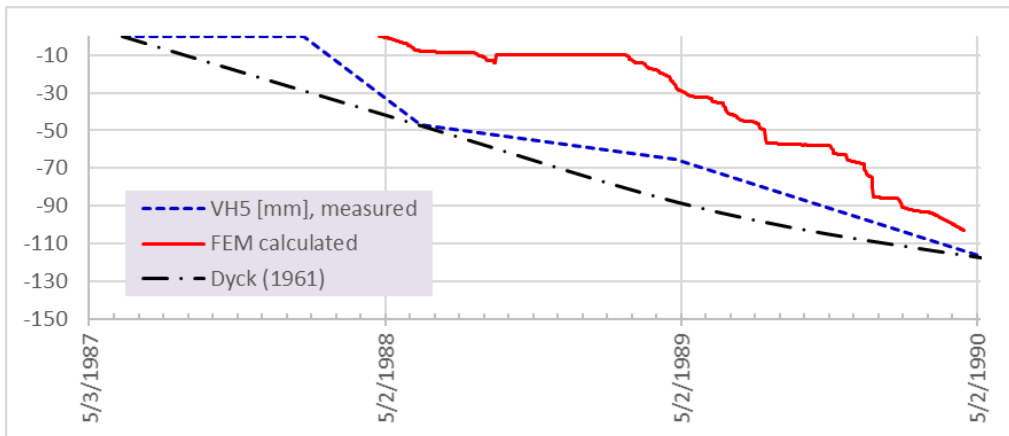


Figure 7. Comparison of calculated and measured horizontal displacements in mm (- downstream direction), in the dam crest (measuring point V5) during the first filling of the reservoir.

In all materials for construction of embankment dams, there is a dependence between stresses, deformations and time. That is, the materials show viscous behavior, and long-term loads on the viscous materials cause significant deformations called "creep" of the material. Figure 7 also shows the secondary horizontal displacements calculated by method of Dyck (1961). The following expression is used to calculate the secondary displacements at the embankment dams after the construction of the dam and the filling of the reservoir:

$$W = \frac{\varepsilon_t H}{100} \quad (1)$$

$$\varepsilon_t = \varepsilon_a + \alpha \ln t \quad (2)$$

Whereas, (W) is displacement in meters, (t) past period in years, (H) is height of dam above terrain, and coefficients (ε_a) and (α) depend on the type of dam and type of displacement.

Horizontal secondary displacements in the direction of the action of hydrostatic pressure are correlated with settlements caused by creep and, according to some authors, their value is about 50% of vertical displacements. Thus, if the mechanical response with the FEM and the empirical concept obtained horizontal displacements in the downstream direction of about 120 mm, the vertical settlement would be approximately 240 mm. For the values of the vertical rising in the crest obtained by the mechanical response with FEM of +150 mm, Figure 8, summed with the vertical creep settlement of -240 mm, we obtain approximately -90 mm, i.e. approximately to the measured settlement of around -100 mm.

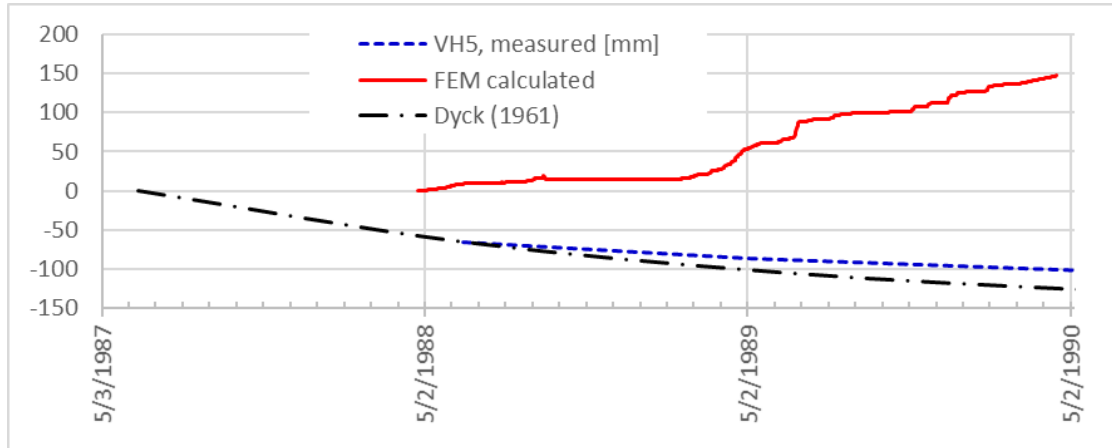


Figure 8. Comparison of calculated and measured vertical displacements in mm (+ elevation, - settlement), in the dam crest (measuring point V5) during the first charge of the reservoir.

2.4 Variation of the water level in the reservoir

The dam states during the variations of the water level in the reservoir from stage 2 to stage 9 (Table 2) are simulated in the time domain of the following numerical experiments:

- Stage 2, raising to normal level with 10 linear increments over a period of 10 days;
- Stage 3 maintenance of normal level with 60 exponential increments over a period of 6,458 days;
- Stage 4 lowering to emergency level with 20 linear increments in a period of 137 days;
- Stage 5 maintenance of emergency level with 30 exponential increments in a period of 3,652 days;
- Stage 6 lowering to remediation level with 30 linear increments over a period of 203 days;
- Stage 7 maintenance of remediation level with 15 exponential increments for a period of 365 days;
- Stage 8, raising to normal level with 30 linear increments over a period of 337 days and
- Stage 9 maintenance at a normal level with 15 exponential increments over a period of 365 days.

The comparison of the estimated (with FEM model and empirical) and the measured horizontal and vertical displacements in the dam crest are shown in Figures 9 and 10.

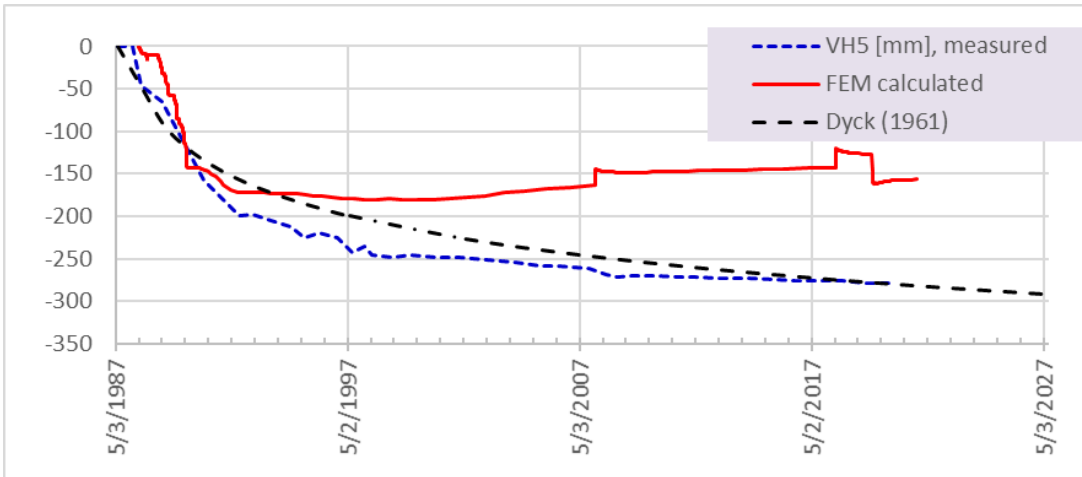


Figure 9. Comparison of calculated and measured horizontal displacements in mm (- downstream), in the dam crest (measuring point V5), during Stage 1 to Stage 9.

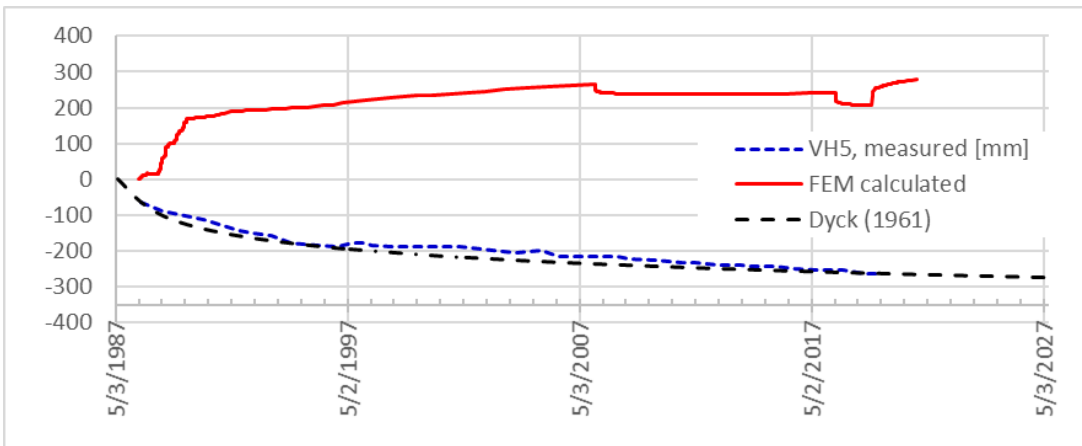


Figure 10. Comparison of calculated and measured vertical displacements in mm (+ elevation, - settlement), in the dam crest (measuring point V5), during Stage 1 to Stage 9.

By extrapolating the displacements in the crest until 2027, under the proper behavior of the dam, a horizontal downstream displacement of 300 mm and a settlement of approximately 300 mm can be treated.

The stress state in the final stage or stage 9, Figure 11, is the initial pre-earthquake state. The coefficient of slope stability of the upstream slope is calculated with the realized stresses with value of $F = 1.6$, i.e. it is greater than the required 1.5, for permanent load.

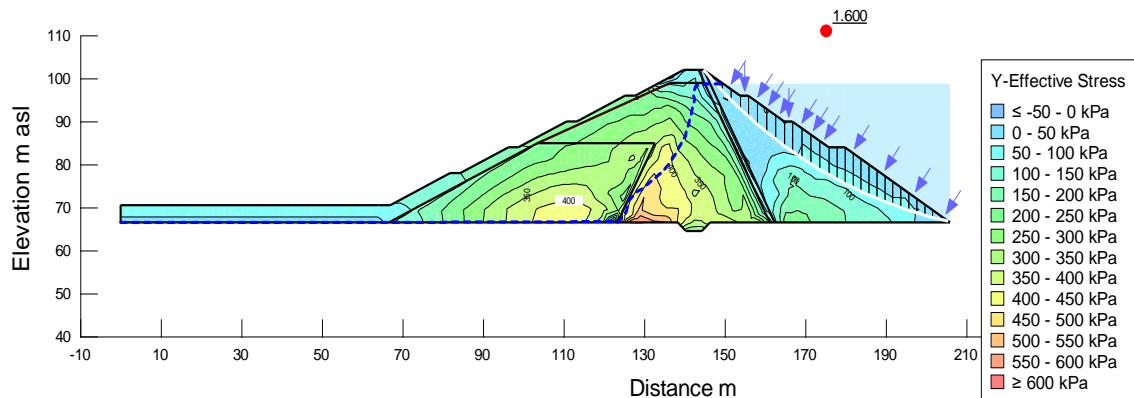


Figure 11. Initial state before earthquake action, distribution of vertical effective stresses, with coefficient of slope stability of the upstream slope $F = 1.6$.

3 DYNAMIC RESPONSE OF THE DAM

3.1 Dynamic material parameters and model for permanent displacements

In the dynamic analysis, a nonlinear model with variable maximum shear modulus is applied for the materials in the dam body, Figure 12. Dynamic analysis is performed with equivalent linear analysis (ELA) with inelastic dynamic parameters of local materials, Figures 13 and 14.

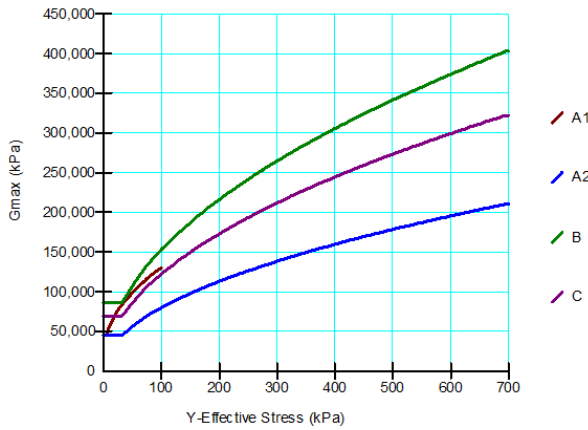


Figure 12. Variable maximum shear modulus $G_{\max} = G(\sigma_y')$ for local materials in the dam body.

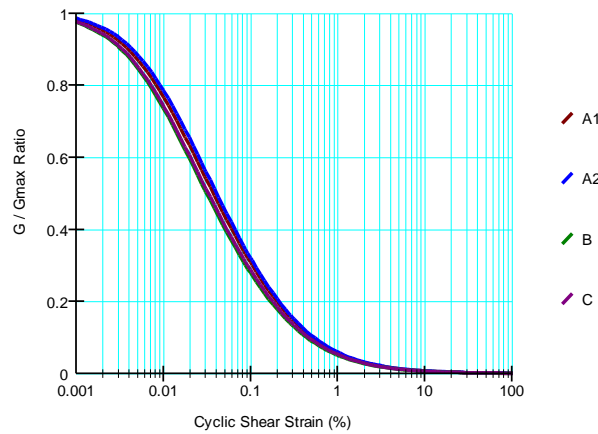


Figure 13. Reduction of the shear modulus with increase of tangential strains for local materials using an equivalent linear model.

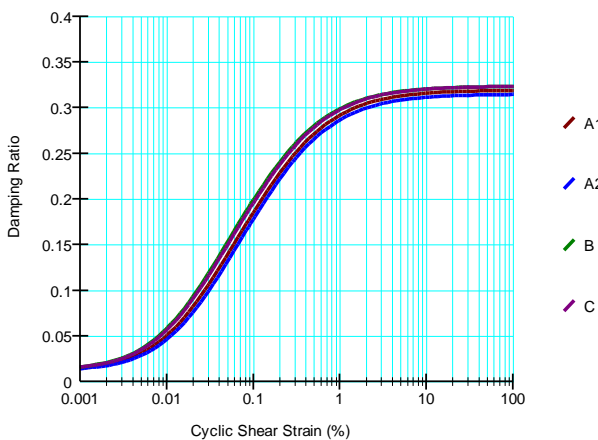


Figure 14. Increase in damping coefficient with increase in tangential strains for local materials using an equivalent linear model.

The approach applied in the present analysis for determination of the permanent deformations during the seismic excitation, for any node within the fill dam, is the method of "Dynamic Deformation Analysis" (DDA), which is successive non-linear redistribution of the stresses [2]. By such method, for geo-medium discretized by finite elements, are calculated deformations caused by forces in nodes, calculated by the incremental stresses in the elements. Thus, by application of non-linear model, for each time step of the dynamic response of the structure [6] is obtained new state of the total stresses and pore pressure. By the differences of the effective stresses in two successive time steps are obtained incremental forces, resulting in deformations, in accordance with the chosen constitutive law for dependence stress - strain. So, for each loading case during the dam's dynamic response are produced elastic and eventual plastic strains. If dynamic inertial forces cause plastic strains, then in the geo-medium will occur permanent deformations. The permanent displacements, at any point in the dam and at the end of the seismic excitation, are cumulative sum of the plastic deformations.

3.2 Eigen periods of the dam

To determine the eigen periods for a certain level of inelastic response of the embankment dam, a dynamic excitation of synthetic harmonic vibration with continuous change of frequencies was used, i.e. with evenly represented frequencies in the interval $f_1 \div f_2 = 0.4 \div 10.0$ [Hz] = $2.5 \div 0.1$ [s]. This harmonic has a maximum amplitude $A_o = 0.001$ g, a total duration $St = 12$ [s], a time increment in the accelerometer $dt = 0.01$ [s], Figure 15. Spectra of excitation response and response, spectral acceleration S_a [g] for damping coefficient $DR = 0.05$, is given in Figure 16 for full reservoir. The dynamic response of the dam is determined using the Quake / W program [3].

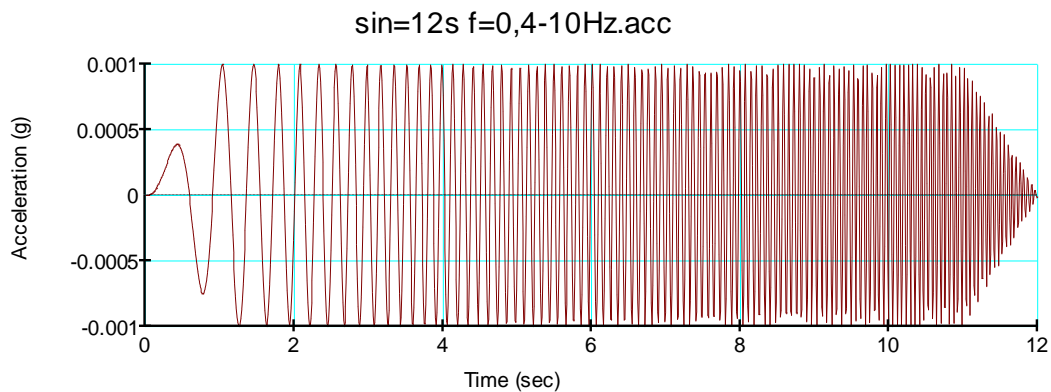


Figure 15. Time history of horizontal accelerations of harmonic vibration with evenly represented frequencies $f_1 \div f_2 = 0.4 \div 10.0$ [Hz], scaled with $A_o = 0.001$ g.

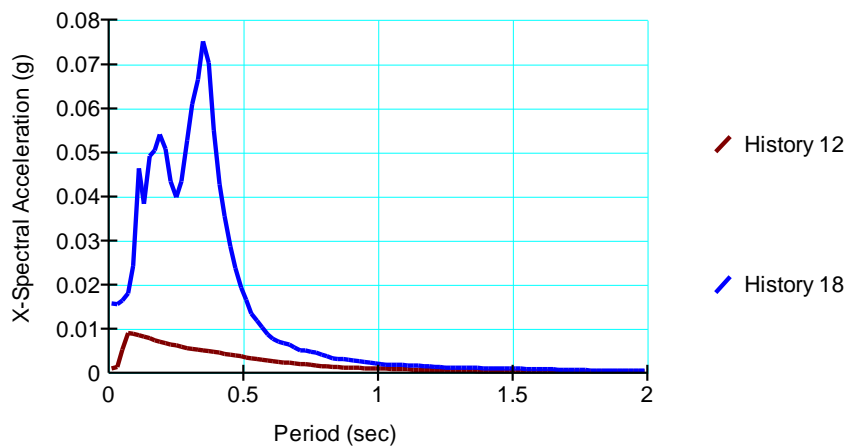


Figure 16. Response spectrum of absolute accelerations in the crest of the dam at full reservoir, caused by harmonic oscillation with low intensity $PGA=0.001$ g, with eigen periods $T_1=0.35$ s, $T_2=0.19$ s, $T_3=0.11$ s.

3.3 Seismology parameters of a strong earthquake

As a basis for generating accelerogram for synthetic earthquake, design spectra are adopted - spectra of elastic response to normalized accelerations from design earthquakes. In the analysis, the design spectra according to the Eurocodes (Eurocode 8, 2003) were used, for type A base for horizontal and type 1 for vertical component. Accelerogram of the horizontal and vertical components of a strong earthquake are given in Figures 17 and 18.

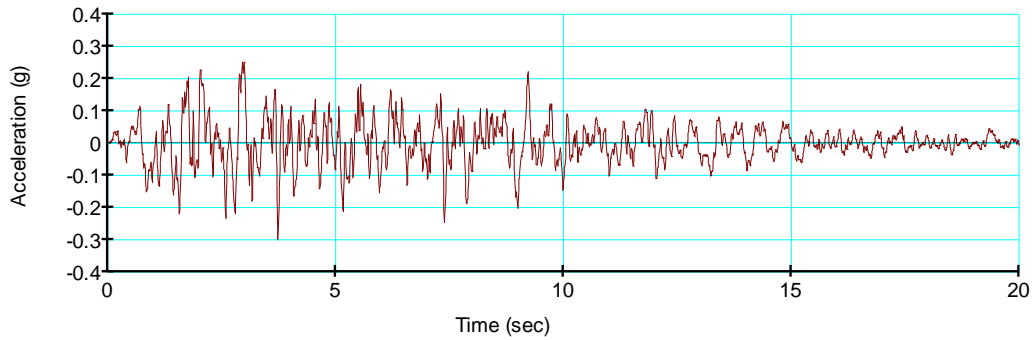


Figure 17. Time history of the horizontal excitation component in the rock foundation for a strong earthquake, $PGA_x = 0.3$ g.

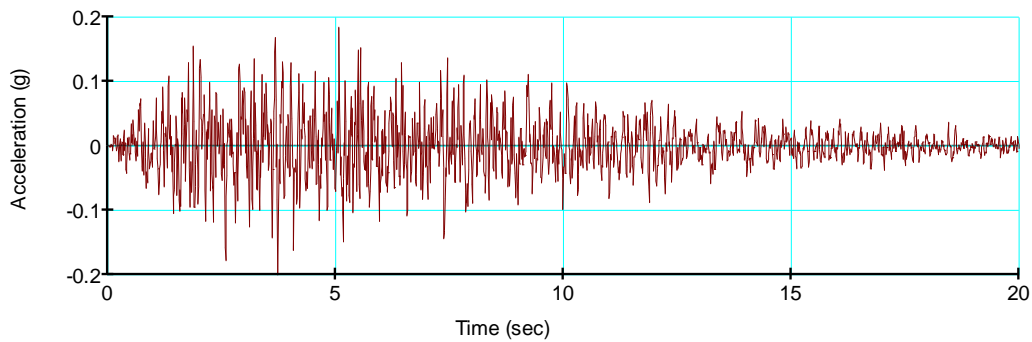


Figure 18. Time history of the vertical excitation component in a rock foundation for a strong earthquake, $PGA_y = 0.2$ g.

3.4 Dam response during a strong earthquake

The horizontal accelerations in the dam crest at occurrence of a strong earthquake are given in Figure 19, and the response spectrum of the accelerations is given in Figure 20.

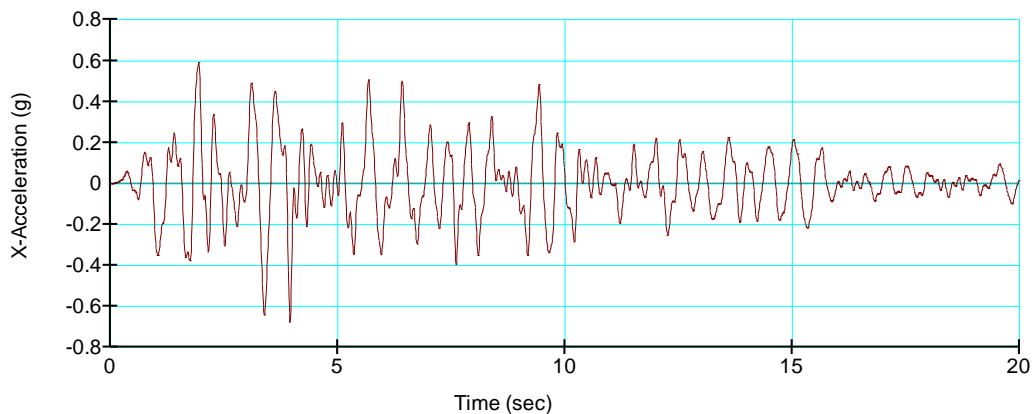


Figure 19. Time history of the horizontal component of the response in the crest of the dam with $PCE = 0.671$ g, under the action of a strong earthquake with $PGA = 0.3$ g.

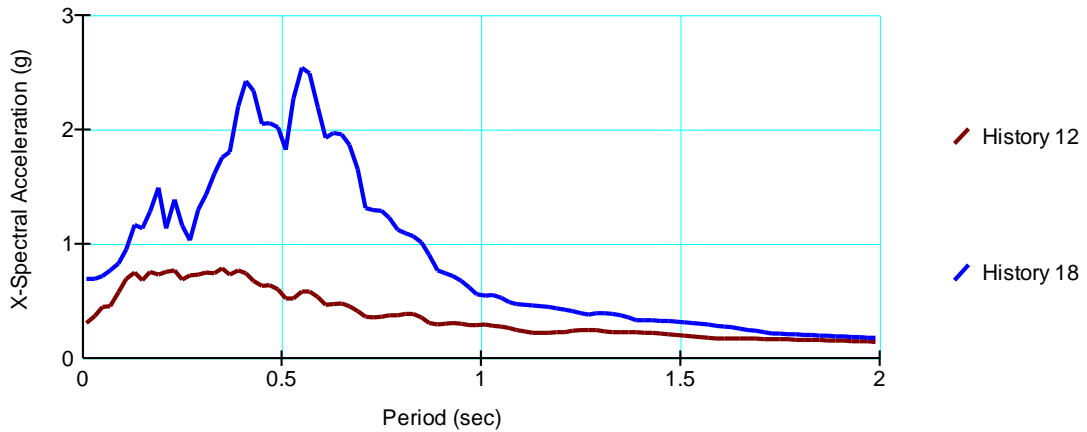


Figure 20. Response spectrum for the accelerations in the base and in the crest of the dam (with $T_1 = 0.55$ s) during the action of a strong earthquake.

The relative displacements in the crest of the dam during the action of this earthquake are given in Figure 21.

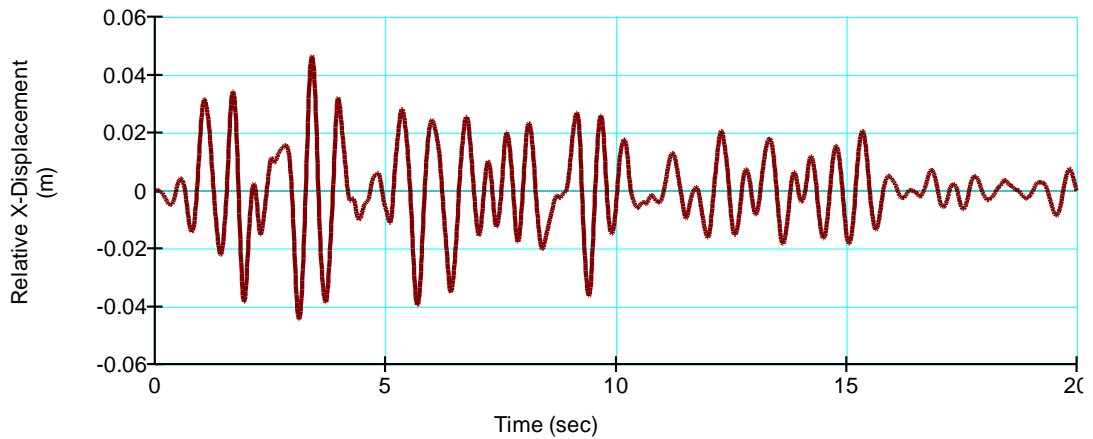


Figure 21. Time history of relative horizontal displacements in the dam crest during a strong earthquake.

The realization of the permanent horizontal and vertical displacements in the crest of the dam during the action of this earthquake are given in Figures 22 and 23, and after the action of the earthquake the permanent XY displacements in the body of the dam are given in Figure 24.

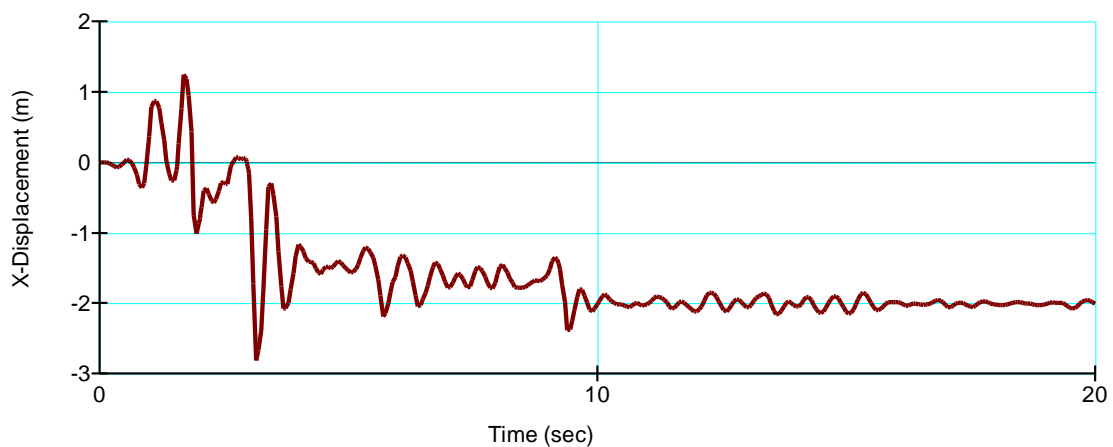


Figure 22. Permanent horizontal displacements in the dam crest (measuring point V5) during a strong earthquake.

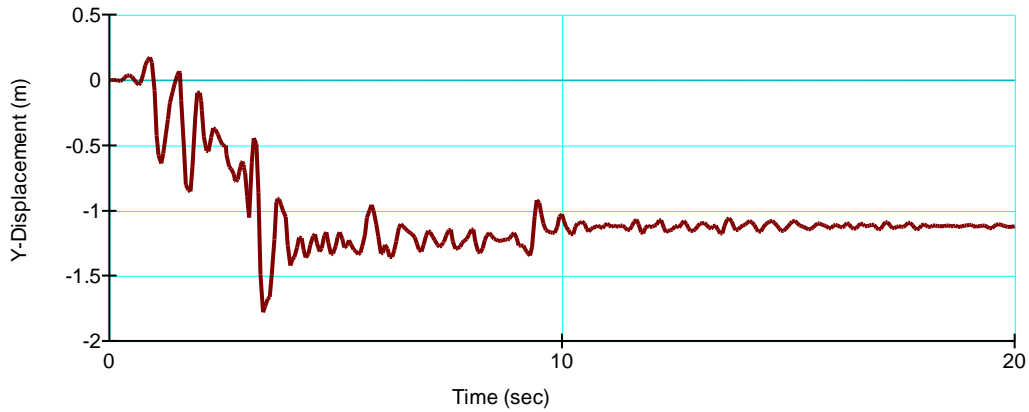


Figure 23. Permanent vertical displacements in the dam crest (measuring point V5) during a strong earthquake.

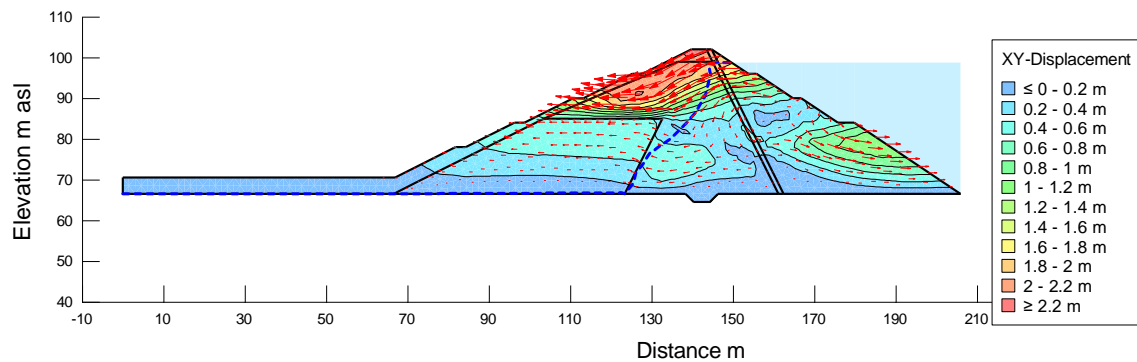


Figure 24. Permanent XY displacements in the dam after the action of a strong earthquake, $XY_{max}=2.3$ m.

4 CONCLUSION

The behavior of the dam during the filling of the reservoir, during the variation of the levels in the reservoir in the service period, and during the seismic excitation is simulated with only one model for structural analysis [6]. This ensures the transfer of the stress state in the analysis, as the initial state for each subsequent load case. The analyzes were performed using the effective stresses, i.e. by simulating of the increase and dissipation of the pore pressure in the drained conditions, with a coupled mechanical and hydraulic response with non-steady seepage.

In the static analysis, for the local materials in the body of the dam, an elastoplastic model with variable modulus of elasticity is applied, with calibrated elastic parameters. Criterion for calibration is the horizontal displacements in the crest of the dam, for the condition of the first filling of the reservoir, to be approximately the same with the measured values, i.e. about -120 mm in the downstream direction.

By extrapolating the displacements in the crest by 2027, under the proper behavior of the dam, a horizontal downstream displacement of 300 mm and a settlement of approximately 300 mm can be treated.

The stability of the dam is analyzed through the coefficient of slope stability (F) with the realized stresses, determined by the FEM model. The determination of coefficient F is performed only for the upstream slope, because with the adopted geometry and layout of the materials, it is obvious that the downstream slope has $F > 2$ for any load case. For the initial condition before the first filling is obtained $F = 1.33 > 1.3$, required for temporary load. For the state of full reservoir is obtained $F = 1.6 > 1.5$, required for permanent load. For the condition of rapid drawdown of the level to remediation elevation (82.0 m.a.s.l.), by applying the Limit Equilibrium Method, a safety coefficient $K_c = 1.373 > 1.3$, required for temporary load, is obtained. For this state, we emphasize that due to the high normal stresses (generated by the hydrostatic load during filling), the safety coefficient F calculated with the realized stresses is extremely higher. The key conclusion from

the static analysis is that the embankment dam, with the adopted geometry and composition of the materials, possesses satisfactory static stability.

The dam's Eigen Periods are determined by the response spectrum when it is excited by harmonic vibration, with equal frequencies from 0.4 to 10.0 Hz, for the initial stress state at full reservoir. For low excitation intensity with $PGA = 0.001$ g, eigen periods $T1 = 0.35$ s, $T2 = 0.19$ s, $T3 = 0.11$ s are obtained. For higher excitation in a strong earthquake with $PGA = 0.3$ g the response of the embankment dam is nonlinear, the stiffness of the local materials decreases with the increased inelastic deformations, which causes an increase of the period of the eigen tone $T1 = 0.55$ s [7]. The values for the base tone ($T1$), determined in the analysis, match the measured values for dams exposed to strong earthquakes in Japan [8,9], which is the best confirmation of the correctness of the adopted dynamic material parameters for nonlinear dynamic analysis.

The values for Dynamic Amplification Factor, where $DAF = PCA / PGA$, where PGA - Peak Ground Acceleration (in the horizontal direction), and PCA e Peak Crest Acceleration in the horizontal direction) are: $0.671 / 0.3 = 2.24$ for a strong earthquake. The response in the crest of the dam corresponds to the registered data on the degree of dynamic amplification of this type of structures under the action of strong earthquakes, [10] and the time history of relative displacements are the key indicator for the correctness of the dynamic analysis.

The permanent settlements in the dam crest, caused by the dynamic inertial forces for the duration of the earthquake, determined by the method of Dynamic Deformation Analysis (DDA), is $Y = - 1.1$ m for a strong earthquake. Regardless of the fact that the subject analysis does not take into account the settlements from additional compaction and reduced stiffness of materials exposed to cyclic action, the total settlement cannot exceed the height of the dam crest (102 m.a.s.l.) to the normal level in the reservoir (98.8 m.a.s.l.).

The key conclusion from the dynamic analysis is that the embankment dam, with the adopted geometry and layout of the materials, has satisfactory seismic resistance. That is, there is no violation of the water resistance of the waterproof body (wide clay core), nor is there a danger of rapid and uncontrolled emptying of artificial lake, because the settlement during the design earthquake with PGA 0.3 g does not overcome the protective height of 3.2 m.

REFERENCES

- [1] Zhvanut P.,, (2022). 16th International Benchmark Workshop on Numerical Analysis of Dams, Theme C, Ljubljana, Slovenia
- [2] Geo-Slope SEEP/W v8, (2017). "Seepage analysis", GEO-SLOPE International Ltd., Calgary, Alberta, Canada.
- [3] Geo-Slope SIGMA/W v8, (2017). "Stress/deformation analysis", GEO-SLOPE International Ltd., Calgary, Alberta, Canada.
- [4] Geo-Slope SLOPE/W v8, (2017). "Stability analysis", GEO-SLOPE International Ltd., Calgary, Alberta, Canada.
- [5] Geo-Slope QUAKE/W v8, (2017). "Dynamic Modeling", GEO-SLOPE International Ltd., Calgary, Alberta, Canada.
- [6] Petkovski L., Tančev L., Mitovski S., (2007) "A CONTRIBUTION TO THE STANDARDISATION OF THE MODERN APPROACH TO ASSESSMENT OF STRUCTURAL SAFETY OF EMBANKMENT DAMS", 75th ICOLD Annual Meeting International Symposium "Dam Safety Management, Role of State, Private Companies and Public in Designing, Constructing and Operation of Large Dams", 24-29 June 2007, St.Petersbourg, Russia, Abstracts Proceedings p.66, CD-ROM
- [7] Park D.S., (2018). Fundamental Period of Embankment Dams Based on Strong Motion Records, Topic Earthquakes - Embankments, USSD 38th Annual Meeting and Conference, A balancing Act: Dams, Levees and Ecosystems, April 3- May 4, 2018, Miami, Florida, USA, CD Proceedings
- [8] Matsumoto N., ..., (2005). "ANALYSIS OF STRONG MOTIONS RECORDED AT DAMS DURING EARTH-QUAKES", 73rd Annual Meeting of ICOLD, Tehran, IRAN, Paper No.: 094-W.
- [9] Fry J.J., Matsumoto N., (2018). Validation of Dynamic Analyses of Dams and Their Equipment, CRC Press/Balkema, Taylor & Francis Group, London, New York, ISBN: 978-0-429-49116-0 (eBook)
- [10] ICOLD, Bulletin 113, (1999). Seismic observation of dams - Guidelines and case studies